

Methodological Notes

**DEMONSTRATION OF LOWER-ORDER MULTIRAY INTERFERENCE FRINGES**

Ya. E. AMSTISLAVSKIĬ

Usp. Fiz. Nauk 92, 345-347 (June, 1967)

**W**E describe here an interference scheme that makes it possible to obtain a multiray interference pattern under unique experimental conditions.

A converging light beam from illuminator O (Fig. 1a) passes through polarizer P and, if necessary, through light filter F and is incident on receiver, R, which has a thin plane-parallel air gap and comprises a set of two glass prisms 1 and 2 that are kept in place and secured with the aid of an elastic mounting. The thickness  $d$  of the air gap between faces AC and A'C' of these prisms is maintained by means of special thin spacers.

To obtain a pattern in reflected light, it is possible to use a set of two identical reversing prisms, using the setup illustrated in Fig. 1b.

The paths of the light rays in the receiver can be seen in Figs. 1a and 1b.

After passing through face AB of prism 1, the light rays are incident on face AC at relatively large angles. The rays whose incidence angles  $i$  are close to  $i_0$  ( $i_0 = \arcsin 1/n$ ) are refracted into the gap at angles  $r$  close to  $90^\circ$ . In this region of the angle  $r$ , the coefficient  $\rho$  of reflection from the gap faces is close to unity, and consequently these faces, even if not specially treated, possess mirror properties suitable for multiray interference.

As a result of multiple reflections from the surfaces, each ray entering the gap at a sufficiently large angle leaves the prism 2 in the form of a beam of parallel rays. Lens L focuses these beams in its focal plane, where the interference pattern is observed. In transmitted light, the path difference  $\Delta$  between the neighboring rays of the interfering beam is given by the formula

$$\Delta = 2d \cos r + \frac{\lambda}{2\pi} (\gamma_1 + \gamma_2). \tag{1}$$

Here  $\gamma_1$  and  $\gamma_2$  are the phase discontinuities occurring upon reflection from the air-glass interfaces. In the case of large  $r$  we have  $\gamma_1 = \gamma_2 = \pi$ . Therefore

$$\Delta = 2d \cos r + \lambda. \tag{1a}$$

In the region of interest to us, where the angle  $r$  is sufficiently large,  $\cos r$  is small and we can obtain a system of interference fringes of low orders at a gap thickness  $d \gg \lambda$ .

The condition for the occurrence of intensity maxima can be written in the form

$$2d \cos r_k = k\lambda \quad (k=1, 2, 3, \dots). \tag{2}$$

The zeroth-order maximum ( $k = 0$ ), which would correspond to the boundary of the region of total internal reflection ( $i = i_0$ ;  $r = 90^\circ$ ;  $\varphi = \varphi_0$ ) is missing from the pattern, since the intensity of the light flux refracted in the gap tends to 0 as  $r \rightarrow 90^\circ$ .

Calculation of the angular displacement  $\psi_k$  of the maxima of lower orders  $k$  relative to the "boundary" of the total internal reflection, and also of the angular distance  $\Delta\psi_k$  between the neighboring maxima of orders  $k$  and  $k + 1$ , leads to the formulas

$$\psi_k = \frac{1}{2} \frac{\cos i_2}{\cos \varphi \cdot \cos i_0} k^2 \left( \frac{\lambda}{2d} \right)^2, \tag{3}$$

$$\Delta\psi_k = \frac{1}{2} \frac{\cos i_2}{\cos \varphi \cdot \cos i_0} (2k + 1) \left( \frac{\lambda}{2d} \right)^2. \tag{3a}$$

The unique feature of the interference produced with this arrangement is that the character of the interference fringes becomes greatly altered when  $k$  increases. The lower-order fringes turn out to be very narrow and sharp. With increasing order  $k$ , an appreciable broadening and smearing of the fringes is observed, owing to the rapid decrease of the reflection coefficient  $\rho$  with decreasing angles  $i$  and  $r$ .

A specially pronounced influence of  $\rho$  on the character of the distribution of the illumination in the interference pattern can be observed by using polarized light. In this case, a very strong change in the con-

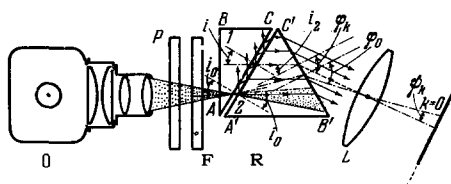


FIG. 1a.

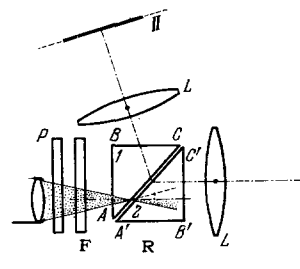


FIG. 1b.

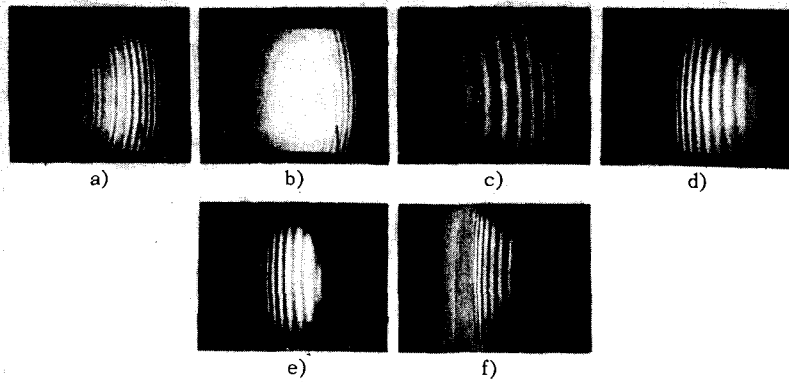


FIG. 2. Overall view of the setup.

trast of the pattern is observed, especially in its central section, on going over from p-oscillations to s-oscillations.

The use of low values of  $k$  in our setup causes its spectral dispersion region  $\Delta\lambda = \lambda/k$  to be large. It therefore becomes possible to observe the pattern not only in monochromatic but also in white light.

In conclusion we note one more feature of the described experiment. Since the layer thickness  $d$  enters in our case into the expression for the path difference  $\Delta$  with a small factor  $\cos r$ , the effect of deviations of the gap faces from plane-parallel is greatly reduced. This makes it possible to obtain a stable interference pattern of satisfactory quality by using a simple elastic mounting without resorting to special methods for its adjustment.

#### DEMONSTRATION OF EXPERIMENT

The main part of the demonstration setup is the receiver, which consists of two prisms: auxiliary prism 1 ( $\angle A = 31^\circ$ ,  $\angle B = 90^\circ$ ,  $AC = 4.8$  cm), and prism 2 ( $A'C' = C'B'$ ,  $\angle C = 62^\circ$ ). Before clamping these prisms, two strips of thin aluminum foil  $6\mu$  thick are placed on opposite edges of face  $A'C'$  of prism 2. It is important that these spacers be placed evenly, without bends, and that their surfaces not be rough. Prism 1 is then placed accordingly on prism 2. The two prisms were tightly clamped to each other and secured with the aid of two rubber gaskets of suitable elasticity, located at opposite bases of the receiver. The receiver  $R$  was mounted on a lifting stage, rotation of which resulted in the required setting and orientation relative to the light beam. To perform experiments in monochromatic light, we used illuminator OI-18 with SVD-120 lamp, and also optical filters to separate the mercury-spectrum lines. The white-light source was an illuminator from an optical bench, with condenser, lens, and 300-watt motion picture projection lamp. The lens  $L$  used in our experiments had a focal length  $F \approx 140$  cm.

It follows from (3) and (3a) that the angular displacements  $\psi_k$  and  $\Delta\psi_k$  are proportional to  $1/d^2$ . Therefore to increase  $\psi_k$  and  $\Delta\psi_k$  it is necessary to decrease  $d$ . To this end we also used in the experiments another receiver  $R_1$ , made of two larger prisms, was similar to  $R$  but without special spacers between the prisms. The air gap was produced in it by the dust particles between the prisms and its thickness was of the order of  $1\mu$ .

The arrangement in Fig. 1a was used for experiments with transmitted light. The arrangement of Fig. 1b makes it possible to obtain a pattern in both transmitted and reflected light (with the angular dispersion region suitably decreased).

When the experiments are demonstrated in a large lecture room it is desirable to display the interference pattern on a remote screen without resorting to a lens. In one such experiment the setup was located at a distance  $l = 5$  meters from a screen measuring  $2.7 \times 1.9$  meters, and the interference pattern covered, completely in part, the full width of the screen, spilling over vertically to the walls of the lecture room. Photographs of some patterns in this type are shown in Figs. 2a, b, c, and d.

The patterns in Figs. 2a and b were obtained by illumination with the line spectra of the OI-18 mercury lamp (without a filter). A polaroid polarizer was used. The photographs show clearly the abrupt changes in the distribution of the illumination which are produced, for the reason indicated above, on going over from s-oscillations (Fig. 2a) to p-oscillations (Fig. 2b).

The patterns in Figs. 2c and d were obtained by using a gap of smaller thickness ( $d \approx 1-2\mu$ ). The first was obtained by using the green line of the mercury spectrum ( $\lambda = 5460.7 \text{ \AA}$ ), and the second by using an incandescent lamp but with a red filter. The orientation of the plane of polarization in both cases was the same (s-oscillations). In white light, the pattern consists of a system of colored fringes—lower-order spectra—the colors in which are quite saturated in the case of the s-oscillations.

The photographs of Fig. 2e and f were also obtained with a thin gap. In this case the receivers were arranged in accordance with the scheme of Fig. 1a and the patterns were observed in the focal plane of the lens L in both transmitted light (in plane I, Fig. 2e) and reflected light (in plane II, Fig. 2f). The patterns were photographed from a small screen

( $0.8 \times 0.8$  m) with the setup illuminated with non-monochromatic red light polarized in the appropriate plane (s oscillations—Fig. 2e, p oscillations—Fig. 2f).

The lower parts of photographs 2a, b, c, and d show traces of the patterns on the edge of the demonstration table.

538.12

## LECTURE DEMONSTRATIONS WITH PULSED MAGNETIC FIELDS

F. Kh. BAIBULATOV

Usp. Fiz. Nauk 92, 347–350 (June, 1967)

**I**F a magnetic field is produced rapidly around a body having electric conductivity  $\sigma$ , then the field will penetrate into the body, within a short time  $t$ , only to a certain skin-layer depth  $l \approx c\sqrt{t/4\pi\sigma}$ . The resultant field gradient will apply on the body a magnetic pressure  $p_m = -\nabla H^2/8\pi$ . This phenomenon is used in plasma accelerators for magnetic compression of the plasma (dc pinch, theta pinch). For a qualitative demonstration of the aforementioned magnetohydrodynamic effects it is very convenient to use metal conductors with suitably chosen mechanical and electrical characteristics.

We describe below demonstrations of radial compression of a metallic tube by a pulsed magnetic field, and also several effects connected with trapping of the field by the tube. A pulsed field was produced by discharging a capacitor bank into a solenoid surrounding the tube. The experiments were performed at first with tubes of 70–80 mm diameter, made of rolled and soldered copper foil 0.15 mm thick. However, more productive experiments were performed with machined duraluminum tubes of smaller diameter. Most employed tubes (T) had a diameter of 20 mm and a wall thickness 0.7–1 mm. With these parameters, the skin layer and the thickness of the wall were of the same order of magnitude; by varying either the wall thickness or the conductivity, it was possible to emphasize or attenuate the effects connected with diffusion of the magnetic field. If the skin layer is smaller than the wall thickness, then the effect of pure external pressure predominates. The resultant clamping of the cylinder produces characteristic folds (Fig. 2a) caused by loss of stability<sup>[1]</sup>. The use of a thinner wall leads to an appreciable diffusion of the magnetic field in the tube. When the field inside the tube reaches its maximum value and begins to drop off, the resultant induced currents retain the magnetic field inside the

tube, so that the internal field exceeds the external one for some period of time, thus causing the inward motion of the wall to give way to outward motion. Photographs taken from the end of the tube have established that the tubes are initially compressed radially at a speed 200–300 m/sec, followed by outward spreading. Figure 2b shows photographs of the tubes after failure, and Fig. 3 shows the calculated time curves for wall thicknesses 0.75 and 1 mm (horizontal hatchures) at an initial capacitor voltage of 4.8 kV. The lengths of the hatchures indicate approximately the inside and outside external diameters. It is convenient to use an epidiascope for a detailed study of the deformed tubes.

By taking oscillograms of the derivative of the current and by suitable calculations, we determined the parameters of the discharge circuit without the tube. The damped-oscillation period was  $T = 80 \mu\text{sec}$  75  $\mu\text{sec}$  with the tube inserted, the total inductance

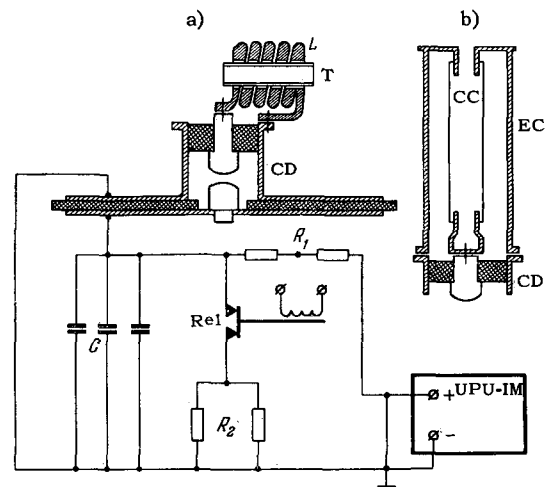


FIG. 1.